Med Biol Eng Comput (2010) 48:1133–1140
DOI 10.1007/s11517-010-0660-8

ORIGINAL ARTICLE

Evaluation of an algorithm for arterial lumen diameter measurements by means of ultrasound

Magnus Cinthio · Tomas Jansson · Anders Eriksson · Åsa Rydén Ahlgren · Hans W. Persson · Kjell Lindström

Received: 26 July 2009 / Accepted: 26 June 2010 / Published online: 16 July 2010

Abstract We have developed an algorithm for arterial luminal diameter measurement by means of ultrasound and evaluated the algorithm on agar vessel phantoms and in vivo. The algorithm utilises relative threshold detection on the inner slopes of the arterial walls before the resolution is improved by solving the equation of a straight line between the samples around the threshold value. Further, correction distances added to compensate for the underestimation when using the inner slopes were found to be 304 μm for the near wall and 415 μm for the far wall. The measured mean diameters of ten consecutive images of 3-, 6- and 9-mm phantoms were 3,006 μm (SD 4), 5,918 μm (SD 1) and 8,936 μm (SD 2), respectively. The mean differences between the images were 0.19, 0.04 and 0.37 μm, respectively. In vivo, the intra- and inter-observer variabilities were −64 μm (2SD 358) and −57 μm (2SD 366), respectively.

Keywords Ultrasonic · B-mode image · Common carotid artery · Arterial mechanics

1 Introduction

Cardiovascular disease is still the major cause of morbidity and premature mortality in the industrial world. Ultrasound is an important tool to gain increased knowledge of cardiovascular diseases. However, new sensitive methods are needed to improve arterial characterization, and to allow early prediction of morbidity and premature mortality. Important parameters in the work to improve existing ultrasound techniques include measurements of the diameter of the arterial lumen and the position of the arterial wall. Examples of methods where these methods are crucial include arterial characterization using calculation of arterial stiffness [1, 2, 15, 19], as well as volume flow measurements using Doppler techniques [27]. Related techniques that would potentially benefit from improved measurement of wall position include wave intensity analysis [26], the combination of images with computational modelling for patient specific diagnosis [21], and in measurements of intima-media thickness [12, 17, 20].

Many automatic and semi-automatic methods for luminal diameter measurements using high-resolution ultrasonic B-mode images have been proposed. One example is the use of sustained attack low-pass filter to identify the edge of vessel walls [13]. One drawback is that this technique needs different parameter values depending on the expected diameter, a problem for which several solutions have been proposed [3, 24]. Further, Newey et al. [18] presented an algorithm that uses neural networks to detect the vessel walls within an ROI. A disadvantage is that the neural network sometimes detects the media-adventitia border instead of the lumen-intima border.

Many of these algorithms are computer intensive [3, 18, 24] and some require manual selection of the arterial wall edge [25]. All methods suffer from the limited resolution achieved in ultrasound images, usually around 0.2–0.5 mm. To improve the resolution, Selzer et al. [23] introduced the sub-pixel edge detection concept. To achieve sub-pixel resolution, they detected the maximum slope position at the

M. Cinthio (✉) · T. Jansson · A. Eriksson · H. W. Persson · K. Lindström
Electrical Measurements, Faculty of Engineering, LTH, Lund University, Box 118, 221 00 Lund, Sweden
e-mail: magnus.cinthio@elmat.lth.se

Å. R. Ahlgren
Clinical Physiology and Nuclear Medicine Unit, Department of Clinical Sciences, Malmö, Lund University, Box 118, 221 00 Lund, Sweden

arterial wall by fitting a parabola to the three largest samples in the gradient curve computed from the intensity values. The position of the maximum of the parabola was regarded as the sub-pixel edge location. Later, Graf et al. [11] made the algorithm more effective by improving the gradient estimation. Recently, Kawakura et al. [14] presented a nonlinear parameter optimization technique which made the estimate more robust.

We have suggested a sub-pixel resolution method that further reduces computational load, and also gives a more robust estimate for sub-optimal images [6]. The algorithm roughly finds the position of the inner slope of each wall using threshold values on the ultrasonic intensity values. Thereafter, the resolution is improved substantially by solving the equation of a line between the two samples around the threshold value of each wall. The refined positions of the walls are then determined from the equations. The detected refined positions are, however, not the true positions of the luminal boundaries, which results in an underestimation of the luminal diameter. The aim of this study was to evaluate the algorithm in vivo and on carefully manufactured phantoms with respect to accuracy and reproducibility, and to determine the magnitude of underestimation of the lumen diameter using phantoms.

2 Methods

2.1 Collection of ultrasound information

All the investigations were performed using a commercial ultrasound system (HDI®5000, Philips Medical Systems, ATL Ultrasound, Bothell, WA, USA). The system was equipped with a 35-mm 5–12 MHz linear array transducer. The data, scan-converted magnitude information, was stored in a cineloop as consecutive frames. The acquisition memory of the ultrasound scanner allowed up to 5.5 s of data to be collected. The cineloop was transferred to a PC for post processing and visualised on the PC in HDILab (Philips Medical Systems, ATL Ultrasound, Bothell, WA, USA), a software designed for off-line cineloop analysis. The images were then exported to Matlab® (The MathWorks Inc., Natick, MA, USA), a software where the arterial diameter measurements algorithm was implemented.

2.2 The phantom

To gain more knowledge about how echoes from the vessel wall behave using high-resolution broadband ultrasound, a simplified physical model of a vessel was manufactured. Because the physical model should be as simple as possible to manufacture, and the fact that we were only interested in investigating the lumen diameter, it was a suitable simplification to only include the echo from one layer at each wall. The physical model was manufactured in agar. The phantom consisted of two different parts: one cylindrical part without sound scattering particles, representing the lumen; and another part containing such particles positioned outside the cylindrical part, representing the vessel walls and the tissue around the vessel. Inhomogeneities in the vessel wall together with the contribution of coherent scattering from the graphite particles produce an apparent wall echo.

The production of the agar solution has been described previously [5], and a similar method was employed by us. First, the solution representing the vessel wall was made, which consisted of 40 g agar (Bacto-Agar, Difco Laboratories, Detroit, MI, USA) and 5 g sodium benzoate per litre water. After the solution was heated to 90°C and clarified, 90 g graphite (type 1.04206.2500, Merck, Darmstadt, Germany) per litre was added and carefully stirred into the solution. The solution was poured into the mould and quickly cooled down in a freezer long enough for the agar to solidify. The mould was cuboid with three iron rods (with measured diameters of 2.99, 5.99, and 8.99 mm) placed horizontally 25 mm below the surface of the mould to create cavities for the vessels. The diameter of the iron rods was measured with an electronic slide-calliper (Rapid, Helios, Messtechnik GmbH & Co., Nidenhall, Germany), which had a stated inaccuracy of ± 7 μm. When the agar with the graphite was solidified, the iron rods were pulled out and the cavities were filled with agar solution without graphite. To minimise the risk of alteration of the diameter during this operation, the outer part was frozen during this operation.

To avoid measurement errors in the ultrasonic method owing to temperature dependence of the speed of sound in the agar [5], the sound speed in the agar solution representing the lumen was measured with a pulse-echo technique on a cuboid reference phantom in conjunction with the measurement of the vessel phantom. The resulting sound speed in the agar during the measurements was 1,490 m/s. The scanner assumed a sound speed of 1,540 m/s and the measurements of the lumen diameter were corrected.

2.3 The measurement algorithm

Let $f(r, c)$ denote the grey-scale information of an ultrasound image with an arterial vessel horizontally oriented (Figs. 1a, 2a), where (r, c) correspond to the coordinates of a pixel in the image plane—r axially and c laterally—with a size of (m, n). The grey-scale information was averaged laterally within a region-of-interest, and the envelope profile $g(r)$ of the vessel was obtained (Figs. 1b, 2b).

$$g(r) = \frac{1}{n}\sum_{i=1}^{n} f(r, c) \quad (1)$$

The positions of the maximum point of each wall were identified in $g(r)$.

Thereafter, the amplitudes of the threshold of each wall ($T_{\text{near wall}}$, $T_{\text{far wall}}$) were determined based on the maximum values. As the absolute level of the maximum echo may vary from person to person and from measurement to measurement, the thresholds were determined as a relative number of the maximum: 20% at the near wall and 10% at the far wall. The values of the percentages were determined empirically so that the beginning of the slope was detected as early as possible but ensuring a level above the noise in the lumen.

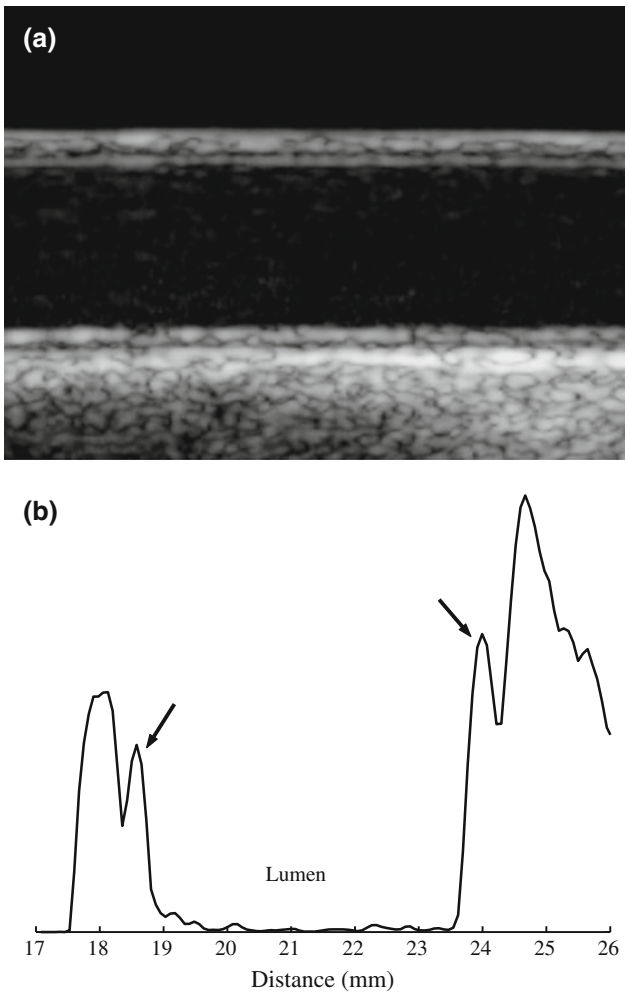

Fig. 1 **a** A scan of the right common carotid. The double-line pattern from the boundaries of the lumen-intima and media-adventitia is clearly visible at both the near and the far wall. **b** The corresponding envelope profile when averaging 5 mm laterally. The *arrows* show the clear echoes from the boundaries between the lumen and the tunica intima of each wall

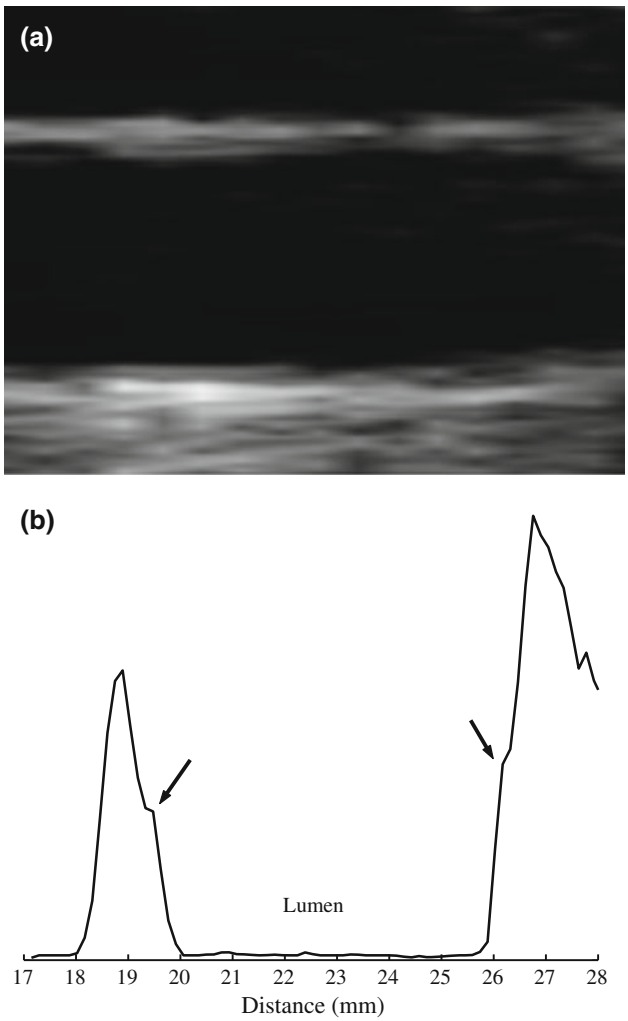

Fig. 2 **a** A B-mode image of the right common carotid during simultaneous tissue Doppler imaging scanning. The double-line pattern from the luminal-intimal and medial-adventitial boundaries is not clearly visible. The settings used one focal point, and allowed a frame rate of 120 Hz. **b** The corresponding envelope profile when averaging 5 mm laterally. The echoes from the boundaries between the lumen and tunica intima are indicated by the *arrows*, but they are almost embedded in the echoes from the medial-adventitial boundaries

A coarse position of the vessel walls was given by finding the first sample that was closest around the thresholds $T_{\text{near wall}}$ and $T_{\text{far wall}}$ at each wall. Because the samples correspond to a pixel in the image, this sets the resolution limit. To further improve the resolution of the measurements, the equation of line ($y = kx + m$) was solved between the two samples around the threshold value of each wall (Fig. 3). The equations of line were easily solved, as the positions and the amplitudes of the samples around each threshold were known. Thereafter, the refined positions of the walls were calculated by finding the intersection between the solved equations and the

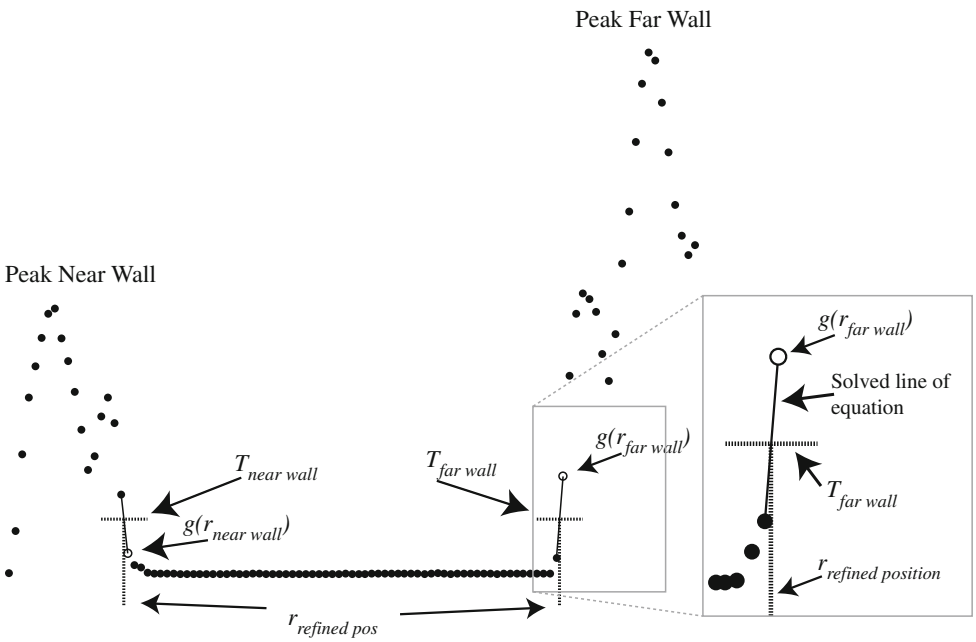

Fig. 3 Vessel profile of the common carotid artery showing the digital representation of the envelope. $T_{\text{near wall}}$ and $T_{\text{far wall}}$ are the calculated threshold values, and $r_{\text{near wall}}$ and $r_{\text{far wall}}$ are the detected vessel wall positions before the improvement of the resolution. In the *right part* of the figure, there is an enlargement of the situation when the resolution of the measurements is improved

thresholds values. The detected refined positions were, however, not the true positions of the luminal boundaries [16]. This resulted in an underestimation of the luminal diameter, the magnitude of which was determined by vessel phantom measurements.

2.4 Phantom measurements

During the measurements, the scanner was set to three transmit focuses, which were placed in level with or just below the lumen. The region-of-interest was zoomed and images sized 20 × 20 mm were collected. This resulted in a spatial quantification of 52 μm in each direction, i.e., a resolution of 19.2 pixels/mm was achieved. The transducer was handheld and the phantoms submerged in a water tank.

The evaluation was divided into four parts. To confirm that the maximum echo of each wall is the most probable placement of the luminal boundaries of the single-layer phantom using high-resolution broadband ultrasound, two different manual diameter measurements were performed with callipers in the B-mode images. Furthermore, the diameters were found by automatic detection of the maximum points of envelope obtained from the B-mode images that were averaged laterally. The diameter was found in envelopes interpolated a factor 1000 using spline interpolation [9]. Moreover, to determine the magnitude of the correction needed using the proposed algorithm the distances between the threshold value positions and the maximum positions of each wall were measured. The interpolated envelope was used in the measurements (see above). Last, to obtain a measure of the repeatability of the proposed algorithm, i.e., to obtain the variation in the measurement due to the differences between consecutive images and movement of the handheld transducer, the lumen diameter was measured on ten consecutive images on each phantom.

2.5 In vivo evaluation

The in vivo recordings were carried out with the subjects in supine position. The common carotid artery was scanned longitudinally, and the vessel was oriented horizontally in the image. Care was taken to minimise the pressure of the transducer in order to not affect the vessel. The in vivo evaluation of the proposed algorithm was divided into two parts. (1) Comparison with manual measurements was carried out on ten healthy normotensive volunteers aged 24–42. (2) Intra- and inter-observer variability measurements were carried out by two experienced technicians on ten males aged 24–34. None of the subjects reported previous cardiopulmonary disease, diabetes, or smoking, and all were free from current medication. All the subjects gave informed consent according to the Helsinki Declaration, and the study was approved by the Ethics Committee, Lund University, Sweden.

The accuracy of the algorithm was compared with a manual identification of the intima position in five images of each of the five subjects (25 images in total) with the intima clearly visible (Fig. 1a), and with the intima embedded in the adventitia echo (Fig. 2a). Manual

identification was carried out on the same envelope curve that the algorithm used. When the intima was clearly visible, the maximum point around the intima was chosen as the lumen boundary (Fig. 1b). In files where the echo from the tunica intima was embedded in the tunica adventitia, the point where a change in the slope occurs (Fig. 2b) was chosen as the luminal boundary. The width of the region-of-interest was approximately 5 mm.

Second, the reproducibility of the algorithm and its performance during simultaneous distension and pulse-wave velocity measurements using tissue Doppler imaging (TDI) were evaluated. The common carotid of ten subjects was examined two times by two different operators. Each examination consisted of four to seven heartbeats, and the diameter at diastole was measured for every heartbeat. The frames corresponding to diastole were obtained from the distension measurements using TDI. The scanner used one focus and low-line density in both the B-mode and TDI. The settings allowed a frame rate of 119 Hz. The width of the region-of-interest was approximately 20 mm.

2.6 Statistics

The accuracy, reproducibility between consecutive frame, and intra- and inter-observer variabilities were evaluated using the method of Bland and Altman [4]. According to this method, the difference between the two repeated measurements was plotted against their mean. In the same graph, the systematic difference as well as the systematic difference ± coefficient of repeatability was plotted. The coefficient of repeatability (CR) was defined as 2 × random difference. The latter shows the 96% confident interval. The systematic difference was defined as

$$\text{Systematic difference} = \frac{1}{2n}\sum_{i=1}^{n} d_i, \tag{2}$$

where d_i is the difference between the examinations of each subject and n is the number of subjects. The random difference was defined as

$$\text{Random difference} = \sqrt{\frac{1}{2n}\sum_{i=1}^{n} d_i^2} \tag{3}$$

Furthermore, the coefficient of variation (CV) was calculated and defined as

$$CV = \frac{\text{Random difference}}{\text{Overall mean}} = \frac{\sqrt{\frac{1}{2n}\sum_{i=1}^{n} d_i^2}}{\frac{1}{2n}\sum_{i=1}^{2n} m_i} \tag{4}$$

where d_i is the difference between the examinations of each subject, n is the number of subjects and m_i is the result of each examination.

3 Results

3.1 Phantom measurements

The measurements confirmed that the most probable placement of the luminal boundaries of the single-layer phantom was on the peak of the echo. The calliper measurements on B-mode images showed that the inner boundaries measurement underestimated the diameter of the vessel phantom on average by 440 μm, whereas the method of measuring maximum echoes overestimated the diameter on average by 40 μm. Two standard deviations were 150 and 90 μm, respectively. When the resolution of the envelope was refined, the automatic detection of the maximum echo of the envelope underestimated the diameter by 29 μm with two standard deviations of 40 μm.

The estimated correction distances that were needed for the proposed diameter measurement algorithm were, on average, 304 μm for the near wall and 415 μm for the far wall. The two standard deviations were 73 and 63 μm, respectively.

The lumen diameters of ten consecutive images of the phantoms were 3,006 μm (SD 4), 5,918 μm (SD 1) and 8,936 μm (SD 2), respectively (Table 1). Figure 4 shows difference against mean for the phantom measurements. The mean difference was 0.19 μm (SD 4), 0.04 μm (SD 1) and 0.37 μm (SD 2), respectively (Table 1); CV was 0.14, 0.01 and 0.02%, respectively (Table 1); and CR for all the three phantoms was 3 μm (Fig. 4).

3.2 In vivo measurements

The mean difference between the automatic algorithm and manual identification of the tunica intima, in the case where the tunica intima was clearly visible, was 130 μm (SD 51). Corresponding result when the tunica intima was embedded in the tunica adventitia echo was 20 μm (SD 98).

The lumen diameter of the common carotid artery at diastole during distension measurement using TDI was 6,623 μm (SD 554). Figure 5a shows difference against mean for the intra-observer variability. The mean difference was −64 μm (SD 179), CR was 263 μm and CV was

Table 1 Summary of the measurement of ten consecutive images of the three phantoms

	3 mm	6 mm	9 mm
Mean (μm)	3,006 (SD 4)	5,918 (SD 1)	8,936 (SD 2)
Mean difference (μm)	0.19 (SD 4)	0.04 (SD 1)	0.37 (SD 2)
CV (%)	0.14	0.01	0.02

CV coefficient of variation

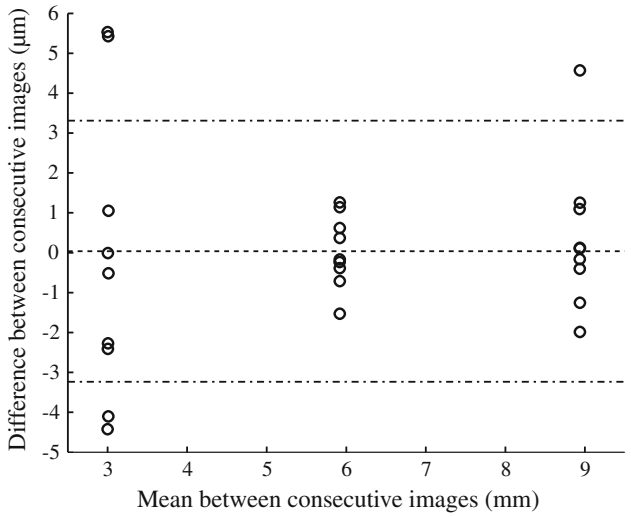

Fig. 4 Difference against mean for ten consecutive measurements of absolute diameter of the 3-, 6- and 9-mm phantoms. The *dashed curve* shows the systematic difference. The *dash-dotted curves* show systematic difference ±2 random difference. Note the different scales on the axes

1.99% (Table 2). The mean standard deviation within an examination of 4–7 cardiac cycles was 74 µm (SD 25). Figure 5b shows difference against mean for the inter-observer variability. The mean difference was −57 µm (SD 183), CR was 258 µm and CV was 1.96% (Table 2).

4 Discussion

We have evaluated an algorithm for automatic estimation of luminal diameter of arterial vessels utilising ultrasonic B-mode images. The algorithm was especially designed to measure the arterial luminal diameter, during distension measurements and pulse-wave velocity measurements [10] using tissue Doppler imaging (TDI), but it can also be used in conjunction with measurement of the recently discovered longitudinal movement of the arterial wall [7, 8] and volume flow measurements [27]. The algorithm average the chosen region-of-interest of the B-mode imaged in the lateral direction. The positions of the near and far wall are thereafter found using threshold values relative to the maximum peak of the wall and the equation of a straight line, respectively.

The phantom study confirmed the observation [16, 28, 29] that the measurements taken at the inside edges underestimate the diameter measurements. The manual calliper measurements of the phantom images also showed that the diameter should be measured around the maximum point of the echo, if it has a single boundary. This was also confirmed when identifying the maximum point in the

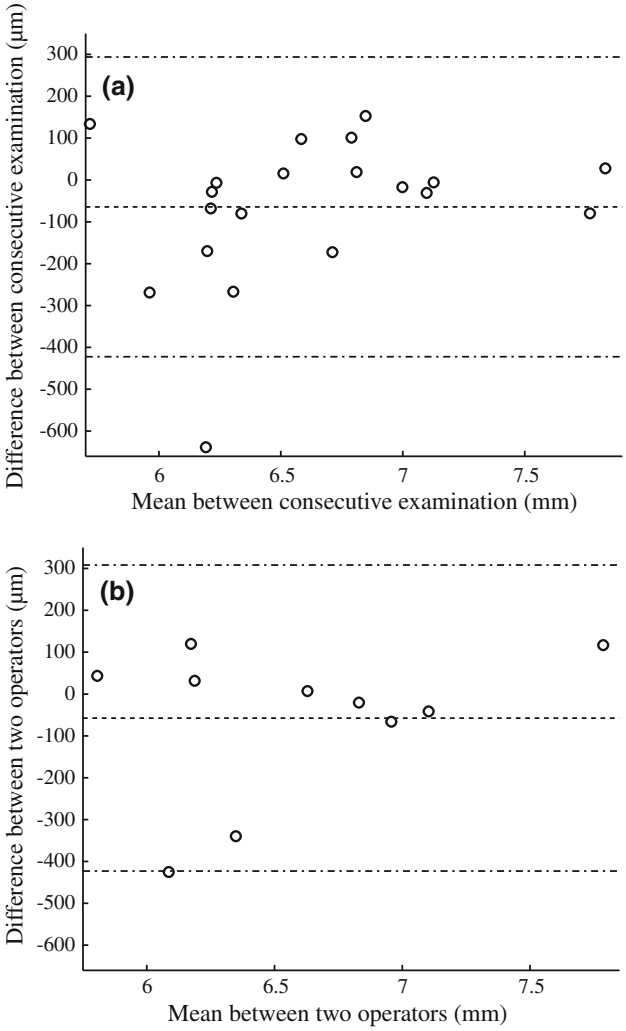

Fig. 5 Different against mean for **a** intra-observer variability and **b** inter-observer variability. The *dashed curve* shows the systematic difference. The *dash-dotted curves* show systematic difference ±2 random difference. Note the different scales on the axes

Table 2 Summary of intra- and inter-variability study of the lumen diameter measurement at diastole on the common carotid artery during simultaneous distension measurements using tissue Doppler

	Lumen diameter
Mean (µm)	6,623 (SD 554)
Intra-observer variability	
Mean difference (µm)	−64 (SD 179)
CR (µm)	263
CV (%)	1.99
Inter-observer variability	
Mean difference (µm)	−57 (SD 183)
CR (µm)	258
CV (%)	1.96

CR coefficient of repeatability, *CV* coefficient of variation

envelope signal. It is therefore more than likely that the true diameter should be measured at the maximum amplitude of the echo if only one boundary is present between the lumen and the tissue, as it is in the phantom. This is also likely in vivo as the distance between the two dominant echoes in the arterial wall is greater than the wavelength of the ultrasonic frequency used in arterial characterisation.

The comparison in vivo between the automatic algorithm and the manual identification of the intima shows that the algorithm works both when the intima is clearly visible and when the intima is embedded in the echoes of the tunica adventitia. The magnitude of the total correction, approximately 0.7 mm, agrees with previous published results [13, 16]. However, the underestimation seems to be somewhat overcorrected. Some of the overcorrection is true when the investigated images were scrutinised, but a part of it is due to the limited resolution in the original envelope. Especially in the files with the intimal echo embedded in the tunica adventitia, it was very hard to identify the true position of the intima manually. Another explanation is that the achieved echo amplitudes from the near and far walls agreed more with the echo levels from the adventitia layer than the intima layer. The magnitude of the measurement error is less than a wavelength, and the accuracy is sufficient for in vivo studies taking into account other uncertainties.

The results of the intra- and inter-observer variability study in vivo show promise. The variability was less than the resolution of the ultrasound system within an examination, between examinations on the same object and between operators (Fig. 5). This performance was achieved on non-optimal B-mode images obtained during simultaneous TDI measurements with a frame rate above 100 Hz. The settings were optimised to suit the TDI measurement, and therefore the line density in the B-mode image was very low. Furthermore, the B-mode image was not visible for the operator as the TDI was overlaid in the image, i.e., the lumen is not perfectly horizontally oriented. Consequently, this often made the intima echo to be imbedded in the adventitia echo when the image was average laterally (Fig. 2).

4.1 Limitations

The in vivo evaluation in this study was conducted on healthy young subjects using as optimal settings as possible. The performance of the algorithm during measurements on older subjects and on subjects with cardiovascular disease as well as using different settings of gain, focus position, TGC, filters and width of the region-of-interest will be further investigated. It has recently been shown that algorithms that utilise the position of first derivative maxima of the ultrasonic intensity of the wall echo in the lumen diameter estimations are more affected by the settings of the scanner than the use of sustained attack filter to identify the edges of vessel walls [22].

A single-layer phantom was used to learn how the lumen diameter should be measured between the echo from the first convex surface interface, and the second echo arising at the concave interface. A more realistic vessel model would have been a double-layer phantom. However, the more complicated manufacturing procedure may affect the accuracy, and also pose a difficulty in determining the origin of the respective echoes.

A limitation of the algorithm today is that it does not take care of tortuous or tilted arteries, i.e., the lateral averaging cause an underestimation of the true lumen diameter if the artery is not horizontally scanned. Further improvements of the algorithm include methods that take care of tilted and tortuous arteries as well as measurement of the lumen diameter change during the cardiac cycle.

5 Conclusions

In conclusion, a novel non-invasive high-resolution algorithm for arterial luminal diameter measurement by ultrasound was evaluated. A vessel phantom in agar was constructed to gain knowledge about the difficult measurement situation, and to calibrate the new algorithm. The results from the in vivo evaluation of accuracy and reproducibility are promising, but further evaluation of the algorithm on aged subjects and subjects with vascular disease are desirable.

Acknowledgments We would like to thank Mrs. Ann-Kristin Jönsson and Mrs. Anita Eriksson for skilful technical assistance. This study was supported by grants from the Swedish Research Council, the Knut and Alice Wallenberg foundation, the Crafoord Foundation and the Royal Physiographic Society in Lund.

References

1. Ahlgren ÅR, Länne T, Wollmer P, Sonesson B, Hansen F, Sundkvist G (1995) Increased arterial stiffness in women, but not in men, with IDDM. Diabetologia 38:1082–1089
2. Balasundaram JK, Banu RS (2006) A non-invasive study of alterations of the carotid artery with age using ultrasound images. Med Biol Eng Comput 44(9):767–772
3. Beux F, Carmassi S, Salvetti MV, Ghiadoni L, Huang Y, Taddei S, Salvetti A (2001) Automatic evaluation of arterial diameter variation from vascular echographic images. Ultrasound Med Biol 27:1621–1629
4. Bland JM, Altman DG (1986) Statistical methods for assessing agreement between two methods of clinical measurement. Lancet 327(8476):307–310

5. Burlew MM, Madsen EL, Zagzebski JA, Banjavic RA, Sum SW (1980) A new ultrasound tissue-equivalent material. Radiology 134(2):517–520
6. Cinthio M, Jansson T, Eriksson A, Persson HW, Lindstrom K (2004). A robust and fast algorithm for automatic arterial lumen diameter measurement with ultrasound. Ultrasonic methods for 2D arterial wall movement measurements. Lund, Lund Institute of Technology, Lund University. ISSN 0346-6221:5/04
7. Cinthio M, Ahlgren ÅR, Jansson T, Eriksson A, Persson HW, Lindström K (2005) Evaluation of an ultrasonic echo-tracking method for measurements of arterial wall movements in two dimensions. IEEE Trans Ultrason Ferroelectr Freq Control 52(8): 1300–1311
8. Cinthio M, Ahlgren ÅR, Bergkvist J, Jansson T, Persson HW, Lindström K (2006) Longitudinal movements and resulting shear strain of the arterial wall. Am J Physiol Heart Circ Physiol 291:H394–H402
9. de Boor C (1978) A practical guide to splines. Springer-Verlag, New York
10. Eriksson A, Greiff E, Loupas T, Persson M, Pesque P (2002) Arterial pulse wave velocity with tissue Doppler imaging. Ultrasound Med Biol 28(5):571–580
11. Graf S, Gariepy J, Massonneau M, Armentano RL, Mansour S, Barra JG, Simon A, Levenson J (1999) Experimental and clinical validation of arterial diameter waveform and intimal media thickness obtained from B-mode ultrasound image processing—fundamental principles and description of a computerized system. Ultrasound Med Biol 25(9):1353–1363
12. Gustavsson T, Liang Q, Wendelhag I, Wikstrand J (1994) A dynamic programming procedure for automated ultrasonic measurement of the carotid artery. Proc IEEE Comput Cardiol 1994:297–300
13. Hoeks APG, Di X, Brands PJ, Reneman RS (1995) An effective algorithm for measuring diastolic artery diameters. Arch Acoust 20(1):65–76
14. Kawamura Y, Yokota Y, Nogata F (2008) Estimation of carotid diameter with heartbeat on longitudinal B-mode ultrasonic images. Conf Proc IEEE Eng Med Biol Soc 2008:3142–3145
15. Kawasaki T, Sasayama S, Yagi SI, Asakawa T, Hirai T (1987) Noninvasive assessment of the age-related-changes in stiffness of major branches of the human arteries. Cardiovasc Res 21(9): 678–687
16. Li S, McDicken WN, Hoskins PR (1993) Blood vessel diameter measurement by ultrasound. Physiol Meas 14(3):291–297
17. Loizou CP, Pattichis CS, Pantziaris M, Tyllis T, Nicolaides A (2007) Snakes based segmentation of the common carotid artery intima media. Med Biol Eng Comput 45(1):35–49
18. Newey VR, Nassiri DK (2002) Online artery diameter measurements in ultrasound images using artificial neural network. Ultrasound Med Biol 28(2):209–216
19. Peterson LH, Jensen RE, Parnell J (1960) Mechanical properties of arteries in vivo. Circ Res 8(3):622–639
20. Pignoli P, Tremoli E, Poli A, Oreste P, Paoletti R (1986) Intimal plus media thickness of the arterial wall: a direct measurement with ultrasound imaging. Circulation 74:1399–1406
21. Ricotta J, Pagan J, Xenos M, Alemu Y, Einav S, Bluestein D (2008) Cardiovascular disease management: the need for better diagnostics. Med Biol Eng Comput 46(11):1059–1068
22. Rossi AC, Brands PJ, Hoeks APG (2009) Nonlinear processing in B-mode ultrasound affects carotid diameter assessment. Ultrasound Med Biol 35(5):736–747
23. Selzer RH, Hodis HN, Kwong-Fu H, Mack WJ, Lee PL, Liu C-R, Liu C-H (1994) Evaluation of computerized edge tracking for quantifying intima-media thickness of the common carotid artery from B-mode ultrasound images. Atherosclerosis 111:1–11
24. Sonka M, Liang W, Lauer RM (1998) Flow-mediated dilation in brachial arteries: computer analysis of ultrasound image sequences. CVD Prev 1(2):147–155
25. Stadler RW, Karl WC, Lees RS (1996) New methods for arterial diameter measurement from B-mode images. Ultrasound Med Biol 22:25–34
26. Sugawara M, Niki K, Ohte N, Okada T, Harada A (2009) Clinical usefulness of wave intensity analysis. Med Biol Eng Comput 47(2):197–206
27. Tortoli P, Bambi G, Ricci S (2006) Accurate doppler angle estimation for vector flow measurements. IEEE Trans Ultrason Ferroelectr Freq Control 53(8):1425–1431
28. Wendelhag I, Gustavsson T, Suurkula M, Berglund G, Wikstrand J (1991) Ultrasound measurement of wall thickness in the carotid artery: fundamental principles and description of computerized analysing system. Clin Physiol 11:565–577
29. Wikstrand J, Wiklund O (1992) Frontier in cardiovascular science. quantitative measurement of atherosclerotic manifestations in humans. Arterioscler Thromb 12(1):114–119